

SYSTEMS WITH H₂O MASER AND 1.3 CENTIMETER CONTINUUM EMISSION IN CEPHEUS A

JOSÉ M. TORRELLES,¹ JOSÉ F. GÓMEZ,² GUIDO GARAY,³ LUIS F. RODRÍGUEZ,⁴ SALVADOR CURIEL,⁵
R. JIM COHEN,⁶ AND PAUL T. P. HO⁷

Received 1998 April 7; accepted 1998 July 14

ABSTRACT

We report continuum (1.3 cm) and H₂O maser line observations, made with the Very Large Array (A configuration), toward the cluster of radio continuum sources in the star-forming region Cepheus A East. The 1.3 cm continuum emission is detected toward HW2, HW3b, HW3c, HW3d, and HW9. In addition, a new continuum source (Cep A:VLA 1), undetected previously, is observed at this wavelength. We detected three spatial clusters of H₂O masers that are associated with the 1.3 cm continuum sources HW2, HW3b, and HW3dii (the brightest component of HW3d), indicating that these objects may harbor an energy source as suggested by Garay and coworkers. The spatial distribution of the H₂O masers with respect to the continuum emission is different in each one of these objects. Toward source HW2 the H₂O masers are spread over $\sim 1''$ and aligned in a direction almost perpendicular to the associated radio jet. In HW3b the H₂O masers are spread over a more compact region ($\sim 0''.5$) and aligned along the major axis of the elongated radio continuum emission. The masers associated with the compact object HW3dii are distributed over a compact region ($\sim 0''.5$) but do not show any clear spatial trend. By comparing the H₂O (this paper) and OH maser distributions in the region, we propose that object HW2, with the strongest H₂O–OH maser activity, could represent the “oldest” young stellar object of the region, while HW3b, with no reported OH maser activity, could be the “youngest” source of these three objects.

Subject headings: ISM: individual (Cepheus A) — ISM: jets and outflows — ISM: molecules — radio continuum: stars — stars: pre-main-sequence

1. INTRODUCTION

Cepheus A is a region of massive star formation (Sargent 1977) located at a distance of 725 pc (Johnson 1957). The region is characterized by the presence of several phenomena such as a rather complex molecular outflow with four lobes (a “quadrupolar” outflow; Rodríguez, Ho, & Moran 1980; Bally & Lane 1991; Narayanan & Walker 1996; Gómez et al. 1998), multiple radio continuum sources (HW sources; Hughes & Wouterloot 1984) located at the edges of massive ammonia clumps (Ho, Moran, & Rodríguez 1982; Torrelles et al. 1985, 1993), Herbig-Haro (HH) objects (Hartigan & Lada 1985; Lenzen 1988), several clusters of H₂O and OH masers (Norris 1980; Lada et al. 1981; Cohen, Rowland, & Blair 1984; Rowland & Cohen 1986; Migenes, Cohen, & Brebner 1992; Torrelles et al. 1996), and infrared sources (Lenzen 1988). In spite of this complexity, a general, although still qualitative, scenario relating these observations has emerged. Most of the HW sources can be interpreted in terms of bright rims of ionized gas externally excited (either photoionized or shock ionized) by a star or stars located at the center of the region. HW2 (the brightest

of the radio continuum sources), which is deeply embedded in high-density molecular gas, would be the main exciting source in the region (Torrelles et al. 1985, 1993; Rodríguez et al. 1994; Garay et al. 1996; Goetz et al. 1998 for further details). However, there are still several points in this region that deserve further study, including (1) which of the HW sources harbor an energy source (see Garay et al. 1996), (2) the nature of the quadrupolar molecular outflow in the region (see Narayanan & Walker 1996 and Gómez et al. 1998), and (3) the relationship between the radio continuum sources and the H₂O and OH masers in the region.

This paper represents the second part of the analysis presented by Torrelles et al. (1996, hereafter TGRCHG96), where we reported simultaneous Very Large Array (VLA)⁸ observations of the 1.3 cm continuum and H₂O maser emission toward the thermal radio jet of Cepheus A HW2 (Rodríguez et al. 1994). In the previous observations, made with an angular resolution of 0''.08 (60 AU), the 1.3 cm continuum emission from source HW2 was resolved into two maxima, as expected in a biconical ionized thermal jet (Reynolds 1986). In addition, a cluster of 28 H₂O maser spots was detected toward HW2. The spatial and kinematic distribution of these masers indicates that the trace is a rotating and contracting circumstellar disk of 300 AU radius perpendicular to the HW2 radio jet (TGRCHG96).

In TGRCHG96 we focused only on HW2, the main energy source of the region. We report and fully analyze now all the continuum and H₂O maser sources detected in Cepheus A East with these VLA observations. In addition to HW2 and its associated H₂O masers, four HW objects (HW3b, HW3c, HW3d, and HW9) and 11 water maser spots were detected. At this particular wavelength and

¹ Instituto de Astrofísica de Andalucía, CSIC, Apdo. Correos 3004, E-18080 Granada, Spain. Present address: visitor at the Instituto Mediterráneo de Estudios Avanzados, CSIC-UIB, Universitat de les Illes Balears, E-07071 Palma de Mallorca, Spain; torrelles@iaa.es.

² Laboratorio de Astrofísica Espacial y Física Fundamental, INTA, Apdo. Correos 50727, E-28080 Madrid, Spain; jfg@laeff.esa.es.

³ Departamento de Astronomía, Universidad de Chile, Casilla 36-D, Santiago, Chile; guido@das.uchile.cl.

⁴ Instituto de Astronomía, UNAM, Apdo. Postal 70-264, DF 04510, México; luisfr@astrosmo.unam.mx.

⁵ Instituto de Astronomía, UNAM, Apdo. Postal 70-264, DF 04510, México; scuriel@astroscu.unam.mx.

⁶ University of Manchester, Nuffield Radio Astronomy Laboratories, Jodrell Bank, Macclesfield, Cheshire SK11 9DL; rjc@jib.man.ac.uk.

⁷ Harvard-Smithsonian Center for Astrophysics, 60 Garden Street, Cambridge, MA 02138; ho@cfaio1.harvard.edu.

⁸ The VLA is a telescope of the National Radio Astronomy Observatory, which is operated by Associated Universities, Inc., under a cooperative agreement with the National Science Foundation.

angular resolution HW3b and HW3d are broken into several subsources. A new object, previously undetected, is identified. We locate with ~ 5 mas precision the water maser positions relative to the radio continuum sources, allowing us to study their relationship. A comparison between the H₂O (this paper) and OH (Migenes et al. 1992) maser spatial distribution is also presented.

2. OBSERVATIONS AND DATA REDUCTION

The 1.3 cm continuum and H₂O maser ($6_{16} \rightarrow 5_{23}$; $\nu = 22235.080$ MHz) observations were made with the VLA of the National Radio Astronomy Observatory (NRAO)⁹ in the A configuration on 1995 July 5. We observed simultaneously two different bandwidths of 25 MHz (seven channels of 3.125 MHz each) and 3.125 MHz (63 channels of 48.8 kHz each), respectively. The broad bandwidth was centered at the frequency of 22285.080 MHz for continuum measurements, while the narrow bandwidth was centered at the frequency of the H₂O $6_{16} \rightarrow 5_{23}$ maser line (22235.080 MHz) with $V_{\text{LSR}} = -8.9$ km s⁻¹. Once the strongest H₂O maser component was identified in a particular spectral channel of the narrow bandwidth, we self-calibrated its signal in phase and amplitude. The phase and amplitude corrections were then applied (as cross-calibration) to both the narrow and broad bandwidth data (see TGRCHG96 for more details of the system parameters and calibration procedures).

In order to study the continuum emission with maximum angular resolution and sensitivity, we produced a map with the task IMAGR of AIPS and the “robustness” parameter set to zero (Briggs 1995). This “robustness” parameter allows us to reach an angular resolution close to that achieved with pure uniform weighting, but with a sensitivity close to that of natural weighting. The resulting angular resolution was 0".08. In order to study weak but extended continuum emission, we also produced a continuum map by convolving the (u, v) data with a Gaussian taper of 950 k λ (half-width at 30%) and natural weighting, resulting in a synthesized beam of 0".2. All the results and analysis of the continuum emission (§§ 3 and 4) are based on these two maps.

With regard to the H₂O maser emission, individual spectral channel maps (63 channels of 48.8 kHz each [0.66 km s⁻¹]) were produced with uniform weighting of the (u, v) data (synthesized beam 0".08). Hanning smoothing was then applied to the cube of 63 channels, giving a final velocity resolution of 1.3 km s⁻¹. This smoothed cube is the one we have used to analyze the H₂O maser emission (§§ 3 and 4).

The uncertainty in the relative positions between the masers and the radio continuum sources is dominated by the contribution from the radio continuum sources and is estimated from its size and signal-to-noise ratio (S/N) [size/2(S/N); e.g., Meehan et al. 1998] to be ~ 5 mas. On the other hand, the accuracy of the absolute positions depends on the accuracy of the position of the phase calibrator and is estimated to be $\sim 0".05$.

3. RESULTS

3.1. 1.3 cm Continuum Sources

A contour map of the 1.3 cm emission observed with a synthesized beam of 0".2 is shown in Figure 1. With this

angular resolution, emission from HW2, HW3d, HW3c, HW3b, and HW9 is detected. Different components of these objects are also detected. Sources in Figure 1 are labeled according to the nomenclature followed by Hughes, Cohen, & Garrington (1995) from detections at other wavelengths. The 1.3 cm continuum parameters of these sources are given in Table 1. A new object (which we have named Cep A:VLA 1), undetected previously, is observed $\sim 1".5$ east from HW9 (Table 1 and Fig. 1). Even though this new source is detected only at the 5σ level, we consider it real since the a priori probability of finding a 5σ noise bump in the map shown in Figure 1 is less than 1%.

HW2, HW3c, and HW3dii (the brightest component of HW3d) are detected in the high-resolution image with a synthesized beam of 0".08. Their positions and flux densities as measured with this particular angular resolution are also given in Table 1. HW2 has been extensively discussed by TGRCHG96, who resolved this source into two maxima (HW2i and HW2ii) plus a faint tail (which we name HW2iii) (Fig. 2a in TGRCHG96; Table 1). The morphology, flux density, and length of this source as a function of frequency are consistent with a biconical ionized thermal jet (Rodríguez et al. 1994; TGRCHG96). Sources HW3c (Fig. 2b) and HW3dii (Fig. 2c) show compact emission, having angular sizes (FWHM) of 0".12 \times 0".08 (PA 78°) and 0".10 \times 0".10, respectively, and represent the two brightest components of the HW3 object.

Since some of the HW sources are known to be variable (Hughes 1988, 1991; Garay et al. 1996), we will not attempt here to make a spectral index study of the sources by comparing the 1.3 cm flux densities with flux densities obtained at other wavelengths and taken at different epochs. We refer to the work by Garay et al. (1996), who determined the spectral indices of most of the HW sources based on observations taken at the same epoch.

3.2. H₂O Masers

We detect 39 H₂O maser spots in the region. These spots are mainly distributed in three clusters coinciding with HW2 (28 spots), HW3d (five spots), HW3b (four spots), plus two other maser spots located, respectively, $\sim 6''$ and $11''$ southwest of HW2. Most of the spots have a single velocity component and line width ≤ 1.3 km s⁻¹. The positions (plotted in Fig. 1), velocity, and intensity of these H₂O masers are given in Table 2. Below we make individual comments on the spatial distribution of the H₂O maser sources.

HW2.—The H₂O maser emission around this object has been extensively studied at different epochs through MERLIN observations by Cohen et al. (1984) and Rowland & Cohen (1986), who have found that this source is the dominant H₂O maser source in the region. Our results also show the dominance of this source in the H₂O maser emission. An accurate comparison of our data with previous H₂O maser observations in terms of intensity and spatial distribution of the H₂O maser spots is not possible given the different velocity resolution, sensitivity, and angular resolution of the various observations.

The H₂O masers around HW2 (Fig. 2a) are mainly distributed in the southeast-northwest direction, almost perpendicular to the radio jet (TGRCHG96). This spatial distribution, as well as the velocity gradients observed along the major and minor axes, led TGRCHG96 to propose that these masers are tracing a rotating and contracting circum-

⁹ The NRAO is operated by Associated Universities Inc., under cooperative agreement with the National Science Foundation.

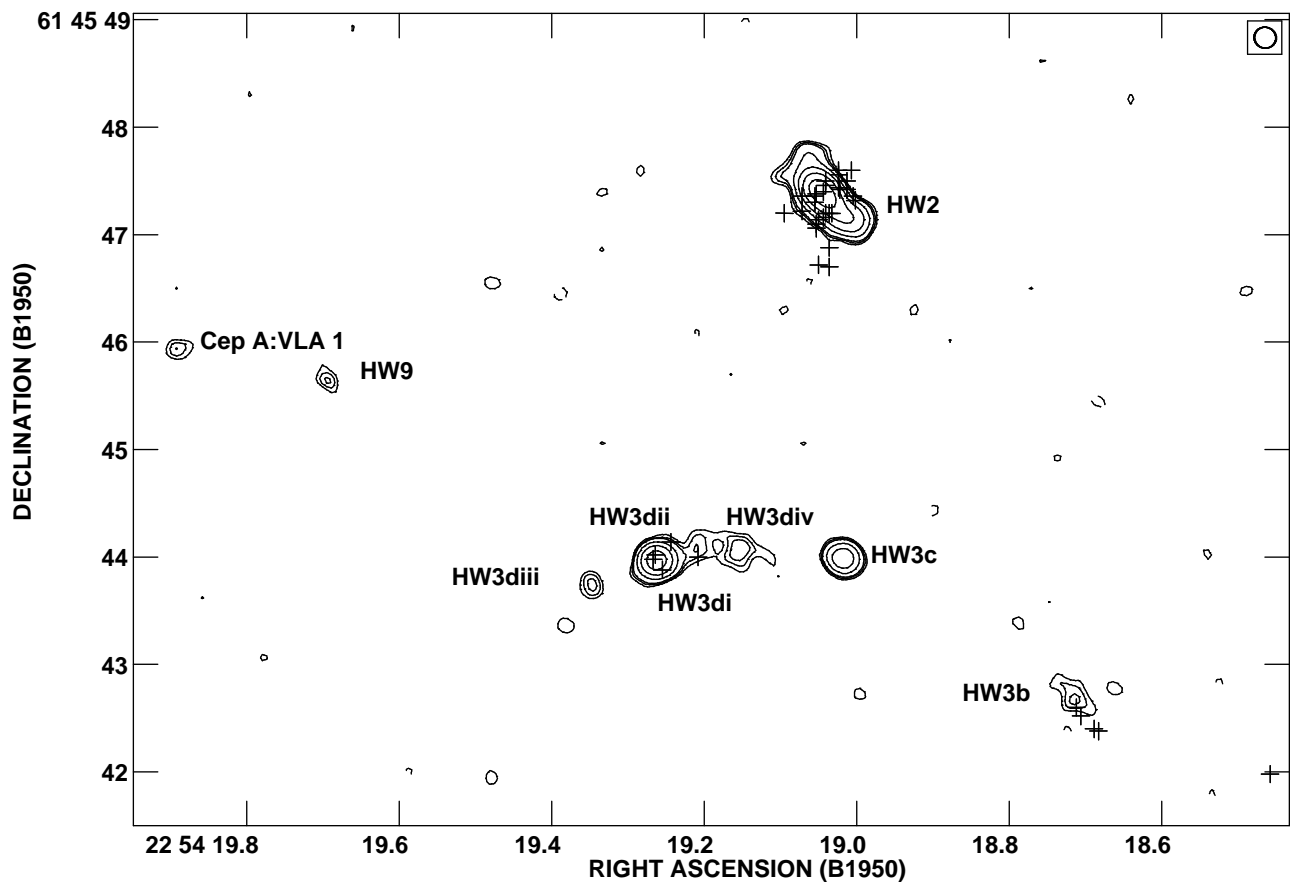


FIG. 1.—The 1.3 cm continuum contour map of the central region of Cepheus A with a beam of $0''.2$ (shown in the upper right-hand corner). HW (Hughes & Wouterloot 1984) sources are labeled according to the nomenclature given by Hughes et al. 1995). Levels are $-3, 3, 4, 5, 10, 20, 40, 80 \times 0.12 \text{ mJy beam}^{-1}$, the rms noise of the map. Crosses indicate the positions of the water masers detected in the region (Table 2; the maser located at $\alpha(1950) = 22^{\text{h}}54^{\text{m}}17^{\text{s}}.923$, $\delta(1950) = 61^{\circ}45'40''.62$ is not plotted here).

stellar disk of 300 AU radius ($0''.4$) perpendicular to the biconical thermal radio jet.

HW3d.— H_2O maser emission from this source has been previously reported by Lada et al. (1981), Cohen et al. (1984), and Rowland & Cohen (1986). Our VLA data show, with higher spatial precision ($\sim 5 \text{ mas}$) than previous observations, that four H_2O maser spots are spatially coincident with HW3dii, while one spot is coincident with HW3di (Figs. 2c and 1). The H_2O maser spots associated with HW3dii are distributed over a more compact region ($\sim 0''.25$ radius) than the corresponding masers around HW2, showing neither a clear spatial trend nor a velocity segregation as a function of position, covering a velocity range of -15.5 to 4.3 km s^{-1} (Table 2).

HW3b.—This source has not been previously reported as associated with H_2O maser emission. The four H_2O maser spots detected in these observations are distributed along an axis of $\sim 0''.5$ size, almost parallel to the elongated radio continuum source (Fig. 2d), without any obvious velocity gradient. In contrast to the H_2O masers associated with HW2 and HW3d, where emission covering a wide velocity range is observed, the masers in HW3b are very closely grouped together in velocity ($V_{\text{LSR}} \simeq -14.8$ to -12.8 km s^{-1}), close to the ambient cloud velocity ($V_{\text{LSR}} \simeq -11 \text{ km s}^{-1}$; Torrelles et al. 1993).

With regard to the two H_2O maser spots located, respectively, $\sim 6''$ ($V_{\text{LSR}} = -10.2 \text{ km s}^{-1}$) and $11''$ ($V_{\text{LSR}} = +0.9 \text{ km s}^{-1}$) southwest of HW2, they are not spatially coin-

cident with any known continuum source. The closest radio source is HW3a (Hughes et al. 1995). HW3a is a highly variable source (see Garay et al. 1996), which coincides with a weak $1 \mu\text{m}$ point source (Lenzen 1988). HW3a is not detected at 1.3 cm continuum at a 3σ level of $0.36 \text{ mJy beam}^{-1}$. The association of these two water maser spots with HW3a is unclear. An H_2O maser spot with $V_{\text{LSR}} \simeq -11 \text{ km s}^{-1}$ undergoing a spectacular flare, doubling its intensity in ~ 5 days, has previously been reported within $0''.2$ of this source (Cohen et al. 1984; Rowland & Cohen 1986).

4. DISCUSSION

4.1. HW Objects with an Internal Energy Source

The physical conditions required to excite H_2O masers, densities of $\sim 10^9 \text{ cm}^{-3}$ and temperatures of several hundred K (e.g., Elitzur 1995), are present characteristically in the circumstellar gas around young stellar objects (YSOs). The fact that now three H_2O maser clusters are coincident, respectively, with the radio continuum emission of HW2, HW3b, and HW3dii, suggests that in addition to HW2, where the presence of an internal source is clearly concluded (zero-age main-sequence B0.5 or earlier star; Torrelles et al. 1985; Rodríguez et al. 1994; TGRCHG96), objects HW3b and HW3dii may also harbor an energy source. These results support the conclusion obtained from spectral index studies by Garay et al. (1996), who derived for

TABLE 1
RADIO CONTINUUM SOURCES AT $\lambda = 1.3$ CM IN CEPHEUS A

SOURCE	POSITION ^a		PEAK (mJy beam ⁻¹)	S_v^b (mJy)
	$\alpha(1950)$	$\delta(1950)$		
Beam = 0'08				
HW2i ^c	22 54 19.036	61 45 47.32	5.9	11.2
ii ^c	22 54 19.050	61 45 47.42	8.0	19.0
iii ^{c,d}	22 54 19.016	61 45 47.16	1.8	8.6
HW3c	22 54 19.019	61 45 43.98	3.0	4.8
HW3dii	22 54 19.264	61 45 43.98	5.2	8.6
Beam = 0'2 ^e				
HW3b	22 54 18.714	61 45 42.66	0.7	2.3
HW3di	22 54 19.210	61 45 44.06	0.6	0.8
iii ^d	22 54 19.154	61 45 44.06	0.8	1.9
iv ^d	22 54 19.346	61 45 43.74	0.7	1.1
HW9	22 54 19.695	61 45 45.66	0.6	0.9
Cep A: VLA 1 ^f	22 54 19.892	61 45 45.94	0.6	1.1

^a Position of the 1.3 cm continuum peak. Units of right ascension are hours, minutes, and seconds, and units of declination are degrees, arcminutes, and arcseconds. The errors in the relative positions depend on the S/N of the emission and are ~ 5 mas. The accuracy of the absolute positions depends on the accuracy of the position of the phase calibrator and is estimated to be $\sim 0'05$.

^b Total flux density.

^c HW2 is resolved into two maxima (HW2i and HW2ii) plus a faint tail (HW2iii). The characteristics of this source are consistent with a biconical ionized thermal jet (see text).

^d These sources were known but were unlabeled by Hughes et al. 1995. We have labeled these known sources extending the nomenclature followed by Hughes et al. 1995 to design other subsources in the region.

^e Sources detected in addition to those shown below by tapering the (u, v) data with a Gaussian function of 950 k λ .

^f New source, undetected previously at other wavelengths.

the integrated HW3d object a positive spectral index $\alpha \simeq 0.3$ ($S_v \propto \nu^\alpha$), consistent with partially optically thick free-free emission and suggesting the presence of an internal YSO. The ultracompact radio continuum emission detected at 1.3 cm (Fig. 2c) further supports this. From our H₂O maser and 1.3 cm continuum observations we conclude that this YSO is located at the position of HW3dii. However, from our data we cannot infer the presence of a radio jet in this object, as suggested by Garay et al. (1996). The emission of HW3dii at 1.3 cm is very compact (undeconvolved size $0'10 \times 0'10$, as observed with a beam of $0'08$; Fig. 2c), with no evidence for elongated emission that would be expected for a radio jet. The elongation of source HW3d reported by Garay et al. (1996) is probably produced by the emission from the nearby sources HW3di, HW3diii, and HW3div and the relatively low angular resolution used by these authors is $\sim 1'2$. When our 1.3 cm continuum data are convolved to an angular resolution of $1'2$, HW3d appears elongated in the same direction as observed by Garay et al. (1996).

With regard to HW3b, a flat spectral index and a size of $1'4 \times 0'5$ (P.A. 49°) at $\lambda = 6$ cm was measured by Garay et al. (1996). With these characteristics the authors could not infer the presence of a thermal radio jet in HW3b ($\alpha \sim 0.6$ would be expected for a thermal radio jet; Reynolds 1986), making it difficult to discern whether this object is internally or externally excited. The observed cluster of H₂O masers toward HW3b suggests now that this object may indeed harbor an internal energy source.

The possibility that HW3b, as well as its associated H₂O masers, are externally shock excited by the wind of HW2 cannot be ruled out, however. In fact, these masers are

closely grouped together in velocity (see § 3.2) and distributed along the same direction of the HW2 radio jet. In addition, the masers associated with HW3b are faint compared with the masers around HW2 and HW3d (see Table 2). High angular resolution observations at millimeter/submillimeter continuum emission toward HW3b could help elucidate the true nature of this object (the detection of this emission would indicate the presence of heated dust around a YSO).

4.2. On the Powering Source(s) and Nature of the Molecular Outflow(s) in the Region

The molecular outflow in Cepheus A was one of the first bipolar outflows reported in the literature (Rodríguez et al. 1980). Even after the numerous studies on this outflow, a clear understanding of its morphology has not yet emerged. When observed in CO with a beam of $\sim 1'$, the molecular outflow is oriented east-west. This particular orientation is also observed in the HH outflows at ~ 1 pc scales, with a prominent ellipse of HH flow toward the eastern regions (Lenzen 1988; Corcoran, Ray, & Mundt 1993). However, when observed with higher angular resolution ($\sim 15''$), the blueshifted and redshifted CO lobes split into two halves, making up a quadrupolar structure (Bally & Lane 1991; Torrelles et al. 1993). Recently, Gómez et al. (1998) observed the HCO⁺ line emission with $3''$ resolution and found that in this molecular tracer the outflow is bipolar, highly collimated at scales of 0.1 pc, oriented at P.A. = 55° – 60° , i.e., close to the orientation of the HW2 radio jet (P.A. 44° – 48° ; Rodríguez et al. 1994; TGRCHG96), and well centered on this object, further supporting HW2 as the main powering source of the molecular outflow.

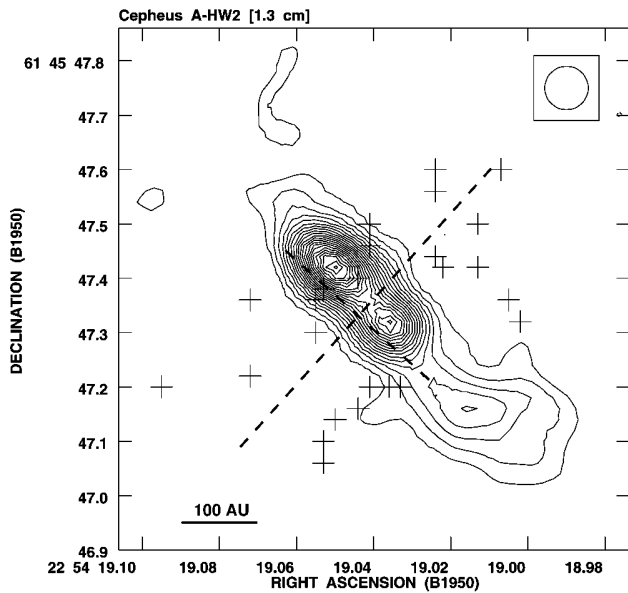


FIG. 2a

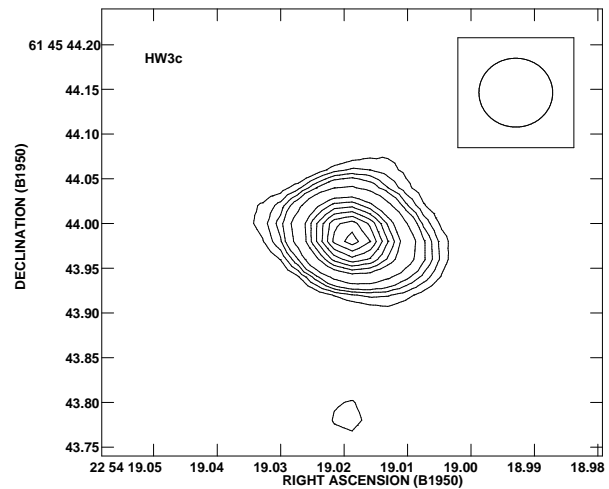


FIG. 2b

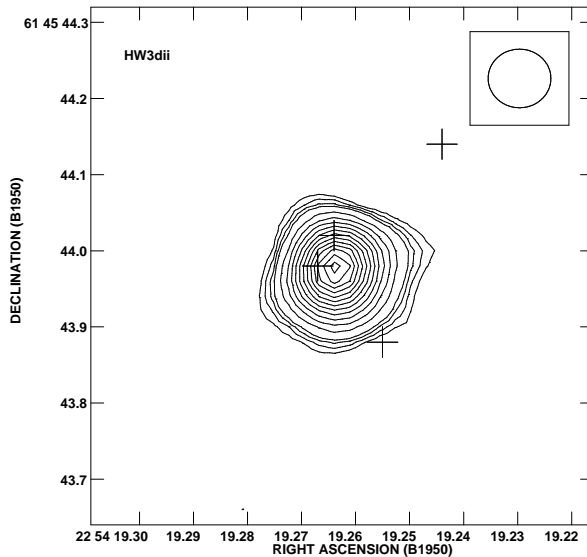


FIG. 2c

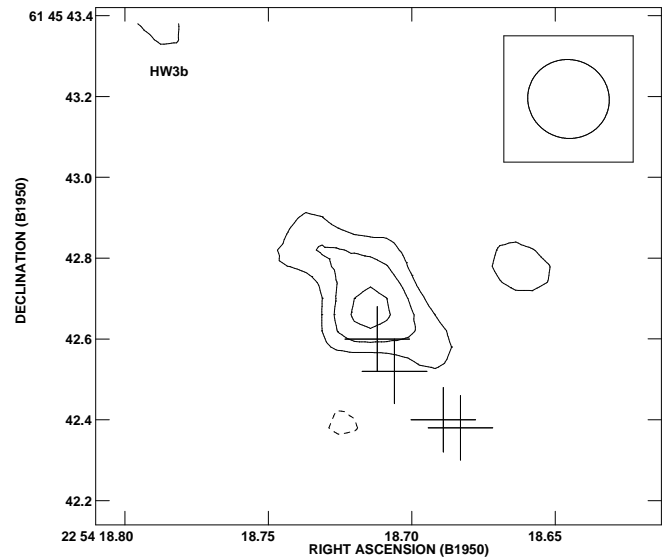


FIG. 2d

FIG. 2.—(a) 1.3 cm continuum contour map of source HW2 with a beam of $0''.08$ (shown in the upper right-hand corner). Crosses indicate the positions of the H_2O masers around this source. Dashed lines indicate the major and minor axes of the disk traced by the maser spots (figure from TGRCHG96). (b) 1.3 cm continuum contour map of source HW3c with a beam of $0''.08$ (shown in the upper right-hand corner). Levels are $-3, 3, 4, 5, 6, 8, 12, 14, 16, 18, 20, 22, 24 \times 0.12 \text{ mJy beam}^{-1}$, the rms noise of the map. (c) 1.3 cm continuum contour map of source HW3dii with a beam of $0''.08$ (shown in the upper right-hand corner). Levels are $-3, 3, 4, 5, 6, 9, 12, 15, 18, 21, 24, 27, 30, 33, 36, 39, 42 \times 0.12 \text{ mJy beam}^{-1}$, the rms noise of the map. Crosses indicate the position of the H_2O masers around this source. (d) 1.3 cm continuum contour map of source HW3b with a beam of $0''.2$ (shown in the upper right-hand corner). Levels are $-3, 3, 4, 5 \times 0.12 \text{ mJy beam}^{-1}$, the rms noise of the map. Crosses indicate the positions of the water masers around this source.

A unified scenario of the activity in Cepheus A East should explain the main characteristics of the observed morphology of the outflow(s) in the region at all scales: a highly collimated bipolar outflow oriented northeast-southwest at small (0.1 pc) scales; a quadrupolar outflow at intermediate (0.5 pc) scales; and a bipolar outflow with a general east-west orientation at large (1 pc) scales, as well as the excitation of the radio continuum sources at the edges of the ammonia clumps. To this end, several interpretations have been proposed by different authors, among them are the following (see Gómez et al. 1998 for a detailed discussion): (1) The outflow is bipolar at the origin of HW2, but it is split and redirected by its interaction with the high-density ammonia clumps, giving rise to the more

extended morphologies (Torrelles et al. 1993); (2) there are two independent outflows, one associated with HW2, producing the northeast-southwest pair of CO lobes and the other one associated with HW3dii, producing the southeast-northwest pair of CO lobes (Garay et al. 1996); and (3) there are two kinds of outflow associated with HW2: an “old” high-velocity and a “new” extreme high-velocity outflow produced by different outbursts from HW2 (Narayanan & Walker 1996). The “old” outflow would be oriented east-west while the “new” one would be oriented northeast-southwest.

Our data give valuable information on scenario 2, although they are not able to discriminate between these three models. In fact, 1.3 cm continuum data have shown

TABLE 2
H₂O MASERS IN CEPHEUS A

POSITION ^a		V_{LSR} (km s ⁻¹)	FLUX DENSITY (Jy)	ASSOCIATED 1.3 CM CONTINUUM SOURCE
α (1950)	δ (1950)			
22 54 17.923.....	+61 45 40.62	+0.9	0.7	HW3a? ^b
22 54 18.458.....	+61 45 41.98	-10.2	0.3	HW3a? ^b
22 54 18.683.....	+61 45 42.38	-12.8	0.05	HW3b
22 54 18.689.....	+61 45 42.40	-14.8	0.3	HW3b
22 54 18.706.....	+61 45 42.52	-13.5	0.2	HW3b
22 54 18.712.....	+61 45 42.60	-13.5	0.2	HW3b
22 54 19.002.....	+61 45 47.32	-9.6	96	HW2
22 54 19.005.....	+61 45 47.36	+0.9	6.7	HW2
22 54 19.007.....	+61 45 47.60	-6.9	1.8	HW2
22 54 19.013.....	+61 45 47.42	-0.3	0.5	HW2
22 54 19.013.....	+61 45 47.50	-1.7	0.06	HW2
22 54 19.022.....	+61 45 47.42	+8.9	0.2	HW2
22 54 19.024.....	+61 45 47.44	-6.9	0.1	HW2
22 54 19.024.....	+61 45 47.56	-14.2	0.08	HW2
22 54 19.024.....	+61 45 47.60	-4.3	0.07	HW2
22 54 19.033.....	+61 45 47.20	-22.1	0.9	HW2
22 54 19.036.....	+61 45 47.20	-15.5	32	HW2
		-11.5	2.1	HW2
22 54 19.036.....	+61 45 46.70	-8.9	603	HW2
22 54 19.036.....	+61 45 46.88	-13.5	0.4	HW2
22 54 19.041.....	+61 45 47.20	-5.0	1.8	HW2
22 54 19.041.....	+61 45 47.46	-24.7	1.2	HW2
22 54 19.041.....	+61 45 47.50	-19.4	1.1	HW2
22 54 19.044.....	+61 45 47.16	-6.9	15	HW2
22 54 19.044.....	+61 45 47.40	-17.5	0.04	HW2
22 54 19.050.....	+61 45 46.72	-8.9	114	HW2
22 54 19.050.....	+61 45 47.14	-9.6	5.2	HW2
22 54 19.053.....	+61 45 47.06	-10.2	3.0	HW2
22 54 19.053.....	+61 45 47.10	-7.6	7.3	HW2
22 54 19.053.....	+61 45 47.38	-27.3	0.5	HW2
22 54 19.055.....	+61 45 47.30	-11.5	0.06	HW2
22 54 19.055.....	+61 45 47.36	-22.7	0.3	HW2
22 54 19.072.....	+61 45 47.22	-25.4	0.2	HW2
		-7.6	0.2	HW2
22 54 19.072.....	+61 45 47.36	-15.5	1.1	HW2
22 54 19.095.....	+61 45 47.20	-22.7	0.06	HW2
22 54 19.208.....	+61 45 44.00	-10.9	0.9	HW3dii
22 54 19.244.....	+61 45 44.14	-10.2	11	HW3dii
22 54 19.255.....	+61 45 43.88	+6.9	1.8	HW3dii
22 54 19.264.....	+61 45 44.02	-15.5	1.0	HW3dii
		-10.2	98	HW3dii
22 54 19.267.....	+61 45 43.98	-5.0	39	HW3dii
		-0.3	34	HW3dii
		+4.3	29	HW3dii

^a Units of right ascension are hours, minutes, and seconds, and units of declination are degrees, arcminutes, and arcseconds. The errors in the relative positions depend on the S/N of the emission and are typically ~ 0.5 mas. The accuracy of the absolute positions depends on the accuracy of the position of the phase calibrator and is estimated to be $\sim 0''.05$. Please note that these masers, if referenced in the future, should be made according to their coordinates and velocity, following IAU guidelines; e.g., H₂O B225417.923 + 614540.62 ($V_{\text{LSR}} = +0.9$ km s⁻¹).

^b The association is unclear. See § 3.2.

that HW3dii does not have a radio jet morphology as HW2 does (§ 4.1). This is expected if HW3dii is powering one of the outflows contributing to the extended quadrupolar morphology observed in the molecular outflow (Bally & Lane 1991). If HW3dii has an associated radio jet it must be at smaller scales than that traced by the angular resolution of our 1.3 cm continuum observations (0''.08) or is much weaker.

4.3. H₂O Maser-OH Maser Distribution

The OH maser emission seen toward Cepheus A East is found to be associated with sources HW2 and HW3d (Norris 1980; Migenes et al. 1992), confirming the presence of an internal energy source in these objects. No OH maser emission has been reported toward HW3b, the other object

thought to contain a YSO. In Figure 3 we plot the positions of the OH masers found by Migenes et al. (1992) together with the positions of the H₂O maser around HW2 and HW3d. The absolute OH maser positions were determined using the positions relative to the Zeeman reference features measured through MERLIN observations (epoch 1989; Migenes et al. 1992), adopting for the last the position measured with the VLA of $\alpha(1950) = 22^{\text{h}}54^{\text{m}}19^{\text{s}}.8$, $\delta(1950) = 61^{\circ}45'44''.1 \pm 0''.2$ (Brebner 1988).

Given the errors in the absolute positions of the OH ($\approx 0''.2$) and H₂O ($\approx 0''.02$; see § 2) masers, an accurate comparison between the OH and H₂O maser positions is not possible at this time. However, these errors do not affect the conclusion that OH masers around HW2 are observed to be spread over a larger ($\sim 2''$) region than the corre-

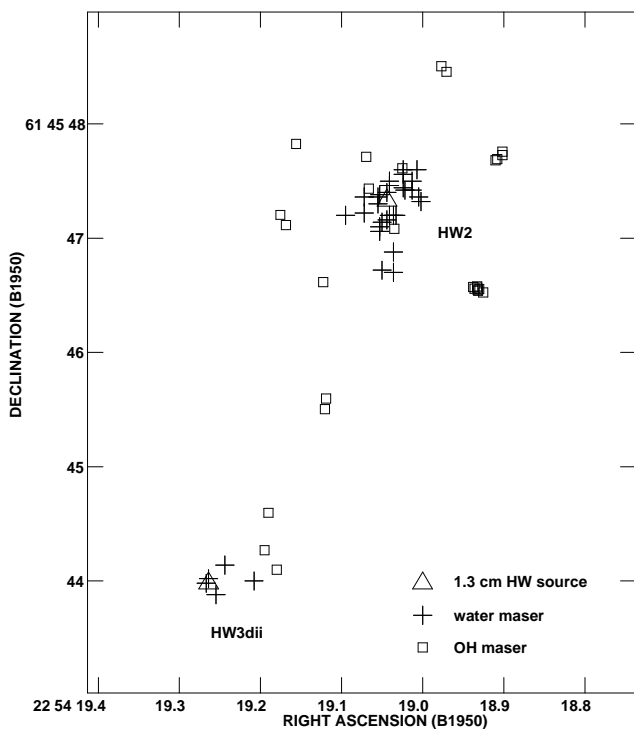


FIG. 3.—Map showing the position of the H_2O masers (crosses; this paper) in the region where OH masers (squares; Migenes et al. 1992) were detected. The positions of the HW2 and HW3dii continuum sources at 1.3 cm are indicated by triangles (this paper).

sponding distribution of the H_2O masers ($\sim 1''$; Fig. 3). This result is consistent with the fact that OH masers seem to form in less dense circumstellar material ($\sim 10^7\text{--}10^8\text{ cm}^{-3}$) surrounding YSOs than H_2O masers do ($10^8\text{--}10^9\text{ cm}^{-3}$) (Forster & Caswell 1989). A possible scenario that would account for the distribution of maser emission in HW2 would be that the H_2O masers are tracing a denser environment, such as the circumstellar disk around HW2 (TGRCHG96), while the OH masers are tracing a less dense gaseous environment, either in expanding gas, as proposed from OH proper motion studies by Migenes et al. (1992), or corresponding to the outer part of the circumstellar disk. Both proper motions studies of the water masers and a more accurate absolute position determination of the OH masers would certainly help to obtain a more detailed understanding of this important issue.

4.4. On the Evolutionary Stages of the YSOs in Cepheus A

As discussed above, at least HW2, HW3dii, and HW3b seem to harbor a YSO. However, both the spatial extent and distribution of the H_2O and OH masers with respect to the continuum emission are different for each of these objects. In fact, in HW2 the H_2O masers are spread over $\sim 1''$ and are aligned almost perpendicular to the radio jet and have a rich OH maser activity (spread over a larger region than the water masers are). In HW3b the H_2O masers are spread over a more compact region ($\sim 0.5''$), aligned along the major axis of the elongated radio continuum emission and are without OH maser activity. Finally, the water masers associated with HW3dii have the tightest spatial distribution ($\sim 0.5''$) but do not exhibit any clear spatial trend. OH maser emission has also been reported toward this source (Migenes et al. 1992).

We suggest that these different distributions could be a consequence of the different evolutionary stage of each associated YSO. According to Forster & Caswell (1989), H_2O masers appear first in high-density circumstellar material ($\sim 10^8\text{--}10^9\text{ cm}^{-3}$), followed later by OH maser emission excited in less dense material ($\sim 10^7\text{--}10^8\text{ cm}^{-3}$). The H_2O –OH maser systems last for about 10^5 yr. After that time, masers disappear (Forster & Caswell 1989). Within this scheme, HW2, with strong H_2O –OH maser activity, could represent the “oldest” YSO of the region, while HW3b, with no reported OH maser activity, could be the “youngest” of these three objects. A similar scenario has also been suggested in W75N(B) and NGC 2071 to explain the radio continuum– H_2O maser systems of the YSOs in these regions (Torrelles et al. 1997, 1998).

Within this evolutionary scenario, we now speculate whether after the YSO of HW2 has been formed, its associated stellar wind could induce the star formation in HW3dii and HW3b by shocking and compressing the molecular gas at the edges of the ammonia condensations. From the hydrogen density derived for the ammonia condensations [$n(\text{H}_2) \simeq (1\text{--}2) \times 10^5\text{ cm}^{-3}$; Torrelles et al. 1993], a free-fall time for the molecular gas of $\sim 10^5$ yr is estimated, which is of the same order as that estimated for the H_2O –OH maser associations (Forster & Caswell 1989). This free-fall time is also on the order of the dynamical age of the molecular outflow associated with HW2 [$(2\text{--}20) \times 10^4$ yr; Narayanan & Walker 1996], indicating that in terms of timescales, HW2 could induce star formation. A scenario like this, with a wind locally shocking and compressing the molecular gas and inducing the star formation, could also modify the morphology of the continuum emission produced by the internal YSO. In this case, it is possible that the observed elongated morphology of object HW3b could be a consequence of this kind of interaction.

5. CONCLUSIONS

Using the VLA in its A configuration we have detected 1.3 cm continuum emission toward different HW sources of the star-forming region Cepheus A East. A new source (Cep A:VLA 1), undetected previously, is also observed. Three clusters of H_2O masers spots were detected in the region. The positions of the water maser spots are determined with milliarcsecond precision relative to the 1.3 cm continuum sources. The three clusters of masers are associated with the 1.3 cm continuum sources HW2, HW3b, and HW3dii, indicating that these objects may harbor a YSO. A comparison between the H_2O (this paper) and OH (Migenes et al. 1992) maser spatial distribution is made. We suggest that HW2, with strong H_2O –OH maser activity, could represent the “oldest” YSO of the region, while HW3b, with no reported OH maser activity, could be the “youngest” of these three objects.

We thank an anonymous referee for many useful and valuable comments. J. F. G. and J. M. T. are supported in part by DGICYT grant PB95-0066 and by Junta de Andalucía (Spain). J. F. G. is also supported by INTA grant IGE 4900506. G. G. acknowledges support from a Chilean Presidential Science Fellowship. S. C. and L. F. R. acknowledge the support of DGAPA, UNAM, and of CONACyT, México. J. M. T. acknowledges the hospitality offered by the Departament de Física of the Universitat de les Illes Balears (Spain) during the preparation of this paper.

REFERENCES

- Bally, J., & Lane, A. P. 1991, in ASP Conf. Ser. 14, Astrophysics with Infrared Arrays, ed. R. Elston (San Francisco: ASP), 273
- Brebner, G. C. 1988, Ph.D. thesis, Univ. Manchester
- Briggs, D. 1995, Ph.D. thesis, New Mexico Inst. Mining and Technology
- Cohen, R. J., Rowland, P. R., & Blair, M. M. 1984, MNRAS, 210, 425
- Corcoran, D., Ray, T. P., & Mundt, R. 1993, A&A, 279, 206
- Elitzur, M. 1995, in Rev. Mexicana Astron. Astrophys. Conf. Ser., Circumstellar Disks, Outflows and Star Formation, ed. S. Lizano & J. M. Torrelles (Mexico: IAUNAM), 1, 85
- Forster, J. R., & Caswell, J. L. 1989, A&A, 213, 339
- Garay, G., Ramírez, S., Rodríguez, L. F., Curiel, S., & Torrelles, J. M. 1996, ApJ, 459, 193
- Goetz, J. A., et al. 1998, ApJ, 504, 359
- Gómez, J. F., Sargent, A., Torrelles, J. M., Ho, P. T. P., Rodríguez, L. F., Cantó, J., & Garay, G. 1998, ApJ, submitted
- Hartigan, P., & Lada, C. J. 1985, ApJS, 59, 383
- Ho, P. T. P., Moran, J. M., & Rodríguez, L. F. 1982, ApJ, 262, 619
- Hughes, V. A. 1988, ApJ, 333, 788
- , 1991, ApJ, 383, 280
- Hughes, V. A., Cohen, R. J., & Garrington, S. 1995, MNRAS, 272, 469
- Hughes, V. A., & Wouterloot, J. G. A. 1984, ApJ, 276, 204
- Johnson, H. L. 1957, ApJ, 126, 121
- Lada, C. J., Blitz, L., Reid, M. J., & Moran, J. M. 1981, ApJ, 243, 769
- Lenzen, R. 1988, A&A, 190, 269
- Meehan, L. S. G., Wilking, B. A., Claussen, M. J., Mundy, L. G., & Wootten, A. 1998, AJ, 115, 1559
- Migenes, V., Cohen, R. J., & Brebner, G. C. 1992, MNRAS, 254, 501
- Narayanan, G., & Walker, C. K. 1996, ApJ, 466, 844
- Norris, R. P. 1980, MNRAS, 193, 39P
- Reynolds, S. P. 1986, ApJ, 304, 713
- Rodríguez, L. F., Garay, G., Curiel, S., Ramírez, S., Torrelles, J. M., Gómez, Y., & Velázquez, A. 1994, ApJ, 430, L65
- Rodríguez, L. F., Ho, P. T. P., & Moran, J. M. 1980, ApJ, 240, L149
- Rowland, P. R., & Cohen, R. J. 1986, MNRAS, 220, 233
- Sargent, A. I. 1977, ApJ, 218, 713
- Torrelles, J. M., Gómez, J. F., Rodríguez, L. F., Curiel, S., Anglada, G., & Ho, P. T. P. 1998, ApJ, in press
- Torrelles, J. M., Gómez, J. F., Rodríguez, L. F., Curiel, S., Ho, P. T. P., & Garay, G. 1996, ApJ, 457, L107 (TGRCHG96)
- Torrelles, J. M., Gómez, J. F., Rodríguez, L. F., Ho, P. T. P., Curiel, S., & Vázquez, R. 1997, ApJ, 489, 744
- Torrelles, J. M., Ho, P. T. P., Rodríguez, L. F., & Cantó, J. 1985, ApJ, 288, 595
- Torrelles, J. M., Verdes-Montenegro, L., Ho, P. T. P., Rodríguez, L. F., & Cantó, J. 1993, ApJ, 410, 202